A STUDY OF THE ELECTRON OPTICAL PROPERTIES OF HEMISPHERICAL DEFLECTION ANALYZERS AIMED AT OPTIMIZING THEIR FRINGING FIELD CORRECTION SCHEMES

Omer SISE[1]

First-order focusing characteristic of hemispherical deflection analyzers (HDAs) is limited due to fringing field at the boundaries of the electrodes. In this paper, we present a systematic study of fringing field effects for different ratios of the gap to mean radius in the range of $0.2 \leq \Delta R/R_m \leq 0.6$ and compare the performance of some useful designs, i.e., ideal HDA, fringing field HDA, Herzog correction, Jost correction, tilted input beam angle, and biased paracentric configuration for resolution improvement.

Keywords: fringing field, real apertures, Herzog, Jost, paracentric analyzer.

1. Introduction

Hemispherical deflection analyzers (HDAs) are irreplaceable as high-resolution monochromators [1] and energy spectrometers of ions and electrons in various atomic collision experiments [2,3], as well as in almost every experimental set-up for surface characterization [4]. By systematically scanning the voltage difference between the hemispheres charged particles with different energies can be made to fly through the fixed distance between slits leading to the formation of an energy spectrum, i.e. number of particles versus energy. In conventional HDAs, the electric field between the hemispheres is generally assumed to be ideal, e.g., the electric field varies as r^{-2}. Sometimes this is a quite good approximation. However, in practice, there are significant fringing field effects at the boundaries of the electrodes. This fringing field increases the trace width, affecting the energy resolution of the analyzer. The fringing field effect becomes more important as the gap between the hemispheres is made large. Therefore, selection of appropriate fringing field corrector for a given HDA is critical in obtaining correct spectrometric results, and final choice of this corrector comes down to a careful consideration of the experimental constraints [5].

In the past, significant effort has been made to eliminate the fringing field effects by using the several correction schemes. The first corrector of overcoming this distortion was devised by Herzog [6], involving the use of condenser plates outside of the analyzer. Oshima et al. [7,8] have also contributed to the development of the Herzog correction in a 127º cylindrical deflection analyzer equipped with a positive sensitive detector (PSD). Nishigaki and Kanai [9] showed that the slits position and sector angle in a 180º hemispherical deflection

[1] Suleyman Demirel University, Turkey, email: omersise@sdu.edu.tr

analyzer must be optimized to find the best focusing condition. Alternatively, Jost [10] proposed an attractive solution for the fringing field correction with attaching plates to the hemispheres, and aligning an aperture or slit between the Jost plates. Hu and Leung [11] modified the position of Jost apertures with a large energy window and flexible size, and showed that this correction scheme was compatible with applications involving PSDs. Another way to eliminate fringing field of real apertures is by using the biased paracentric configuration. This kind of geometrical arrangement was first proposed by Benis and Zouros [12]. In this and our subsequent papers [13-15] it has been shown that the first-order focusing properties and hence energy resolution of an HDA can be improved by taking advantage of its entry fringing field. This is accomplished by changing the entry bias and position from their conventional values to new values.

An important consideration in selecting the geometry of an HDA is the ratio of the gap to mean radius $\rho = \Delta R/R_m$ which determines the maximum entrance angle accepted by the analyzer [16,17]. The aim of this work is to come up with a suitable modeling for fringing field correctors, and to simulate and eventually optimize its performance including trace width and tilted beam angle required to refocus the beam in the exit plane for a variety configurations of ρ in the range of $0.2 \le \rho \le 0.6$. The objective of our modeling is also to provide a guide for the design of any fringing field correctors for HDAs.

2. Design Consideration

In an ideal HDA, first investigated by Purcell [18], the deflecting electrostatic field is formed by two concentric spherical surfaces of radii R_1 and R_2 at potentials V_1 and V_2 where 1 and 2 refer to inner and outer hemisphere, respectively. The radial electrostatic field produced between the two spherical surfaces varies as $1/r^2$. For a pass energy of E_0 to travel along the central trajectory ($R_m = (R_1 + R_2)/2$), the potentials given by Eq. 1 must be applied to the inner and outer hemispheres of the analyzer [19].

$$qV_i = E_0\left\{1 - \frac{\gamma}{\xi}\left[\frac{R_0(1+\xi)}{R_i} - 1\right]\right\} \qquad (i = 1,2), \tag{1}$$

where the parameter $\xi = R_0/R_\pi$ called as 'paracentricity' characterizes the asymmetry of the HDA, R_0 and R_π are the entrance and exit radius of the beam, and γ is the biasing parameter. A conventional centric HDA is seen to have $\xi = 1$ and $\gamma = 1$.

One of the most important features of an analyzer is energy resolution. For the purpose of simulations of energy analyzers, the base energy resolution of HDAs is given by the generic formula:

$$\frac{\Delta E_B}{E} \approx \frac{(\Delta r_\pi)_{computed}}{D_\gamma}, \tag{2}$$

where Δr_π is the trace width and D_γ the energy dispersion defined as $D_\gamma \equiv E\,\partial r_\pi/\partial E$ for central trajectory ($r_0 = R_0$, $\alpha = 0$), differing in energy by ΔE are spatially separated by ∂r_π (dispersed) along the dispersion direction in the image plane where the first-order focusing occurs (analogous to Barber's rule for homogeneous B-field spectrographs). The change in r_π for a finite change in entrance conditions from those for which the hemispheres are tuned ($r_0 \rightarrow R_0 \pm \Delta r_0/2$, $E \rightarrow E \pm \Delta E/2$, $\alpha \rightarrow 0 \pm \alpha$) is given by [15]

$$\Delta r_\pi = |M|\Delta r_0 + D_\gamma \frac{\Delta E}{E} + P_1\alpha + P_2\alpha^2 . \tag{3}$$

Here, magnification (M), dispersion (D_γ), and first- and second-order angular aberration coefficients (P_1 and P_2) are tabulated for most known electrostatic analyzers. Best (smallest) resolution can be obtained for larger D_γ and smaller or zero P_1 and P_2. Typically, an ideal HDA has only first-order focusing ($P_1 = 0$) which is important for good transmission. If an input electrostatic lens is used then it is possible that the lens focus size (Δr_0) is smaller than the width of the entrance slit (virtual aperture). If the pre-retardation mode is used in the lens then angular aberration terms usually becomes larger due to the Helmholtz-Lagrange Law [20].

The equations of motion in the ideal HDA can be derived from the Lagrangian in spherical coordinates and simplified considerably. However, there are no mathematical models that can accurately calculate fringing field for HDAs. In order to obtain an accurate estimate of the fringing field, numerical calculations have to be performed. Using the different analyzer geometries, a computer model was created to simulate the trajectories of electrons through the 180º hemispherical deflection analyzer and to verify and optimize the fringing field correction considering real aperture, Herzog correction, Jost correction, and biased paracentric configuration, as illustrated in Fig. 1.

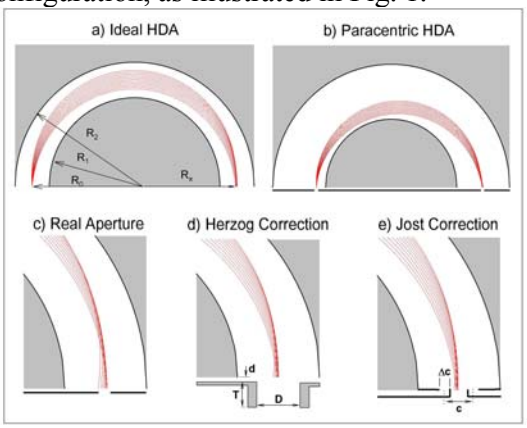

Fig. 1. Schematic diagram of a hemispherical deflection analyzer for (a) an ideal field HDA, (b) biased paracentric HDA, and some electron trajectories of a centric HDA near the exit plane for (c) real aperture, (d) Herzog correction with $d/\Delta R = 0.15$, $T/D = 1$ and $D = 0.74\ \Delta R$, and (e) Jost correction with $c = \Delta R/3$ and $\Delta c = \Delta R/10$.

SIMION v8.1 ion optics program based on the five-point relaxation technique of the finite difference method was used for modeling and analysis. A user-written Lua workbench program was also used to optimize the trace width and the tilted beam angle of HDAs**.**

3. Results and Discussion

3.1. Ideal and fringing field HDA

A hemispherical deflection analyzer acts like a filter allowing only a particular energy width ΔE to be transmitted. The trace width Δr_π in the dispersion plane is useful analyzer characteristic closely related to the base energy width. Fig. 2a shows the electron trajectories in an ideal HDA with input angles α from -5º to +5º in steps of 1º, and we assumed no energy spread for the electrons entering the analyzer. The normalization of radial position r is indicated as r/R_m in all trajectories. It clearly shows that the focus plane moves to the exit plane of the HDA with a small spread (Δr_π) which depends on the mean radius R_m and maximum half-angle α_{max}. For electron beams with three different E/E_0 ratios, focusing are achieved for each electron beam at the exit plane with $\alpha = \pm 1$º and 0º (Fig. 2b). The arriving position of electrons depends linearly on their energy with a constant spread (chromatic aberration). The relationship between the entrance angle and position is shown in Fig. 2c. One can obtain from the analysis of the trajectories in an ideal HDA that $M = -1$ (inverted image), $D = 2R_m$, $P_1 = 0$, and $P_2 = -D$.

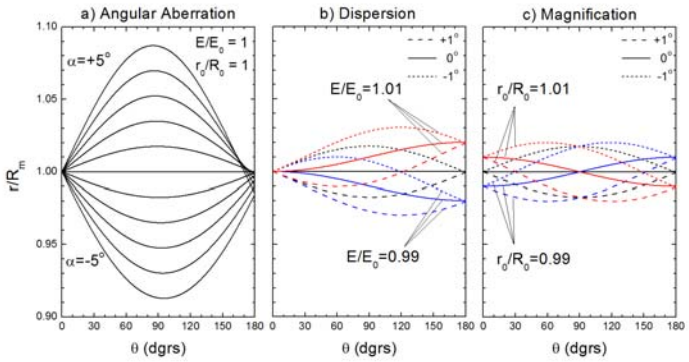

Fig. 2. First order focusing in the dispersion plane of an ideal HDA and some of electron trajectories with different entrance angle α, position r_0, and incident energy E.

The main purpose of using apertures (or slits) at the entrance and exit of the analyzer is to increase the energy resolution. However, close to the edges of the real apertures, inhomogeneous field (thus the distortion of the equipotential

lines) is present that deflects the electrons according to their input angle α. As depicted in Fig. 3, the analyzer with real apertures was not able to bring the electron beam to a well defined focus. In conventional HDAs, fringing field generally creates an image which possesses a positive first-order and negative second-order angular aberration terms, which means that each electron trajectory at the image plane has an offset at the dispersion plane. The terms P_1 and P_2 are affected by the fringing field while magnification and dispersion remain almost constant. The reason is that the fringing field is curved and there will be radial and tangential electric field components which are different from the ideal spherical field as shown in Fig. 4a. As the ratio of the gap to the mean radius ρ increases, the radial electric field component deflects the beam more strongly in the dispersive direction, and as a result, the beam will defocus (see Fig. 4b). The correction of the fringing field effects is, therefore, very important for HDAs with a large inter-radial distance.

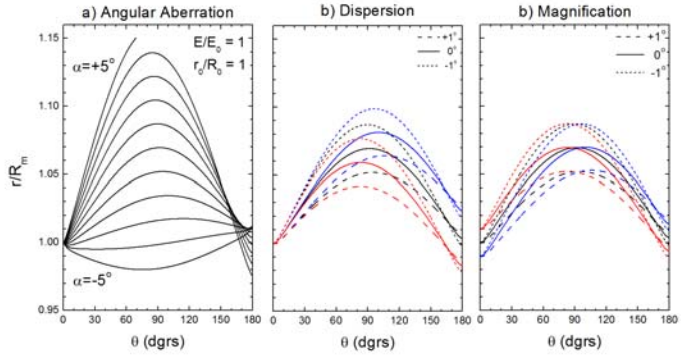

Fig. 3. The same as Fig. 2, but for the fringing field HDA. The image displacement due to the fringing fields is clearly seen.

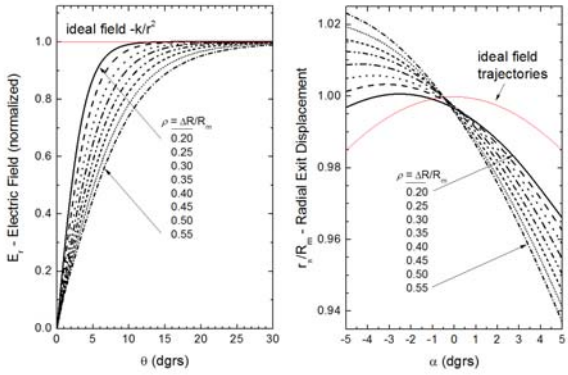

Fig. 4. Normalized radial electric field as a function of orbit angle θ (left) and normalized radial exit displacement as a function of entrance angle α (right) for fringing field HDAs with different values of $\Delta R/R_m$.

3.2. Herzog correction, Jost correction and tilted the input beam angle

Fringing field correction is a key problem on the way to high resolution. In the literature, two different design concepts have been followed for compensating the fringing field effects of real aperture at the exit and entrance of the analyzer: Herzog correction (Fig. 1d) and Jost correction (Fig. 1e). In principle, the usage of the Herzog correction with $d/\Delta R = 0.15$, $T/D = 1$ and $D = 0.74\Delta R$ can significantly improve the operation of the analyzer. As shown in Fig. 5b, the spread of the beam reduces substantially for Herzog correction when it is compared to real aperture configuration (Fig. 5a). By employing an arrangement of the Jost corrector that satisfied the conditions, $c = \Delta R/3$ and $\Delta c = \Delta R/10$, the ideal trajectories were nearly accomplished (Fig. 5c).

Refocusing of the electron beam can also be achieved by tilted all input beam angles α outward by α_{tilt} being assigned to the angles of divergence in the dispersive direction. This optimization also works for Herzog and Jost corrections, allowing a larger acceptance angle and hence a higher transmission efficiency. Figures 5d-f show the electron trajectories through the analyzer with different entrance angles after the rotating the input angles by an optimized α_{tilt} for obtaining similar bundle as in the truly ideal field. For example, to compensate the fringing field effect in Herzog correction, the entrance angle has to be shifted about -1.5º. In this case, the traces are nearly ideal compared with the same traces in a truly ideal field. According to these results, the exit positions without tilting are asymmetric with respect to the central electron trajectory ($\alpha = 0$). With an optimized value of α_{tilt}, electron trajectories show ideal performance and exit positions are symmetric in the exit plane.

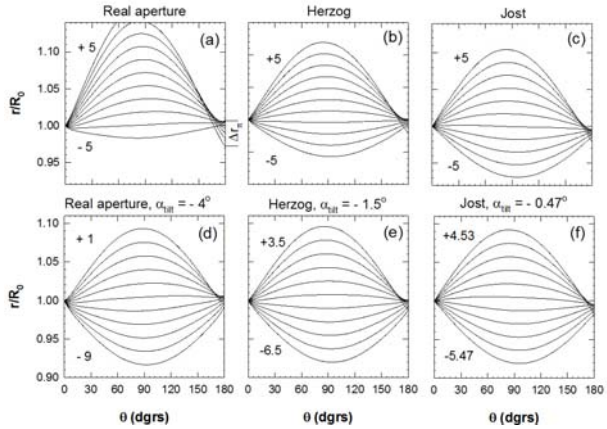

Fig. 5. Calculated electron trajectories with various incident angle ranges from -5º to +5º for real aperture, Herzog correction and Jost correction before (a-c) and after (d-f) the refocusing the electron beam with an input angle tilted outward (negative direction) by α_{tilt}. Here, the ratio of gap to mean radius is $\rho = 1/3$.

Fig. 6a indicates how the trace width of real apertures, Herzog correction, and Jost correction disperses as continuous function of ρ. The ideal trace width is also plotted for reference, which is constant ($\Delta r_{\pi\text{-}ideal} = 2R_0\,\alpha_{max}{}^2 = 1.523$ mm) for all ρ. It should be noted that by varying ρ, for instance, decreasing ρ about 0.2, the simulations yield trace width in a minimum range. The spread of the beam is found to increase with increasing ρ. Then, the trace widths in Fig. 6a could be reduced as the input beam angle is varied, and focusing at the exit position could be restored for different ρ by tilting the input beam angle outward (α_{tilt}). Simulations are in agreement with the values of previous studies for $\rho = 0.2$ [9], 0.3 [21] and 0.6 [11] that they reported these values as -2.6º, -3.4º, and -6.5º, respectively.

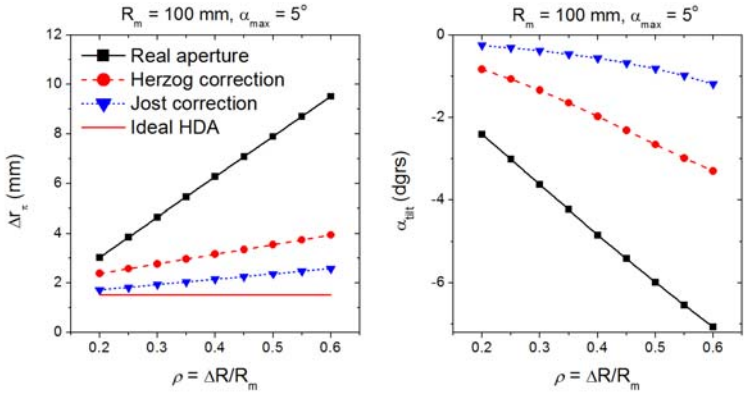

Fig. 6. Trace width (Δr_π) in the exit plane and tilted beam angle, α_{tilt}, required to refocus the electron beam as a function of ρ for real aperture, Herzog correction, and Jost correction. The trace width is defined as the maximal width of the image for a point monoenergetic source.

3.3. Biased paracentric configuration

The biased paracentric configuration has a variable entry position R_0 and an entry bias (controlled by the biasing parameter γ, see Eq. 1). This is a simple and effective way of minimizing the effects of the fringing field on the optical properties of HDAs. Given a specific configuration ($R_1 = 70$ mm and $R_2 = 130$ mm), the principle of this correction was illustrated in Fig. 7 for two different entry positions, $R_0 = 85$ mm and 115 mm, respectively. At each entry position, a search for the corresponding optimum values of γ and/or α_{tilt} minimizing Δr_π was performed. The spread of the beam at the exit plane in Figs. 7a and 7d can be significantly improved when α_{tilt} (in Figs. 7b and 7e) or γ (in Figs. 7c and 7f) is optimized. For $R_0 = 85$ mm, optimal combinations of (γ, α_{tilt}) are ($\gamma = 1.64$, $\alpha_{tilt} = 0$) or ($\gamma = 1.0$, $\alpha_{tilt} = -8.5$º) (the former is referred to as γ-focusing, the latter as α-focusing). For $R_0 = 115$ mm, optimal combinations of (γ, α_{tilt}) are ($\gamma = 0.49$, $\alpha_{tilt} = 0$) or ($\gamma = 1.0$, $\alpha_{tilt} = -7.5$º). Obviously, the radial spread of the paracentric entry

HDAs has been significantly reduced after the optimization process. Here, the dependence of radial position on the deflection angle are presented for the HDA with $\rho = 0.6$, but can be expressed for other values of ρ.

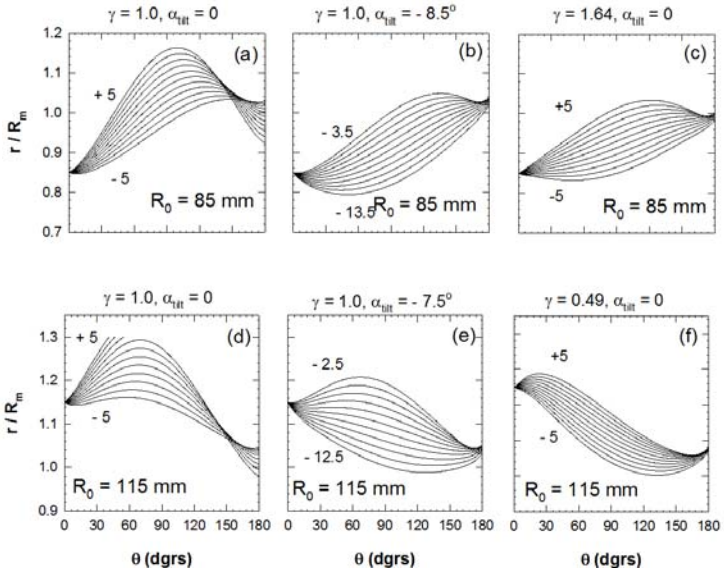

Fig. 7. Computer simulations of electron trajectories for two biased paracentric configurations with (a)-(c) $R_0 = 85$ mm, and (d)-(f) $R_0 = 115$ mm with different biasing parameter γ and α_{tilt}.

We see in Fig. 8 that both biasing γ and α_{tilt} are doing the same thing, i.e. symmetrizing the trajectory bundle around the central ray and thus restoring the spread. This would result in an increase in intensity of about three times when compared to Jost correction (see Fig. 6a for $\rho = 0.6$), in addition to the advantage of a large-gap HDA that is required for the use of PSDs. Moreover, this method does not introduce complicated shapes for the correcting electrodes and because no additional potentials are required.

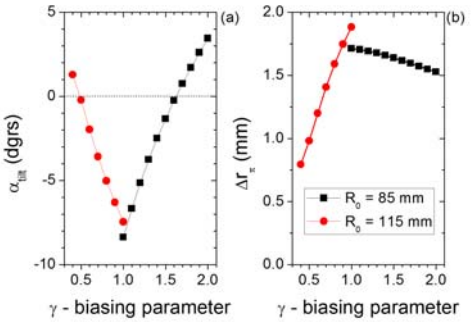

Fig. 8. Plotting trace width (Δr_π) and tilted beam angle (α_{tilt}) versus γ for two entry positions, $R_0 =$ 85 mm and 115 mm, respectively.

4. Conclusions

In this work, we have investigated the electron optical properties of hemispherical deflection analyzers with several fringing field correctors using ray tracing method, considering real apertures, Herzog correction, Jost correction, and biased paracentric configuration. The axis of the beam tilted outwards has been also considered for resolution improvement. Two important issues were addressed in detail. First, the analyzer geometry and its fringing field corrector should be optimized to minimize undesired distortion in the ideal field approximation. Such an optimization improves the energy resolution with the stability of the current. Second, both biased paracentric configuration and tilting input beam angle must be considered, as it directly influences the focusing properties. The results suggest that selection of appropriate fringing field correctors in the design stage of HDAs for high resolution is always recommended. Furthermore, it would be interesting to compare the properties of a double hemispherical analyzer with biased paracentric configuration since many aberrations will be cancelled out due to the symmetry of the double-type analyzer.

REFERENCES

[1] *E Essers, G Benner, T Mandler, S Meyer, D Mittmann, M Schnell, R Höschen*, "Energy resolution of an Omega-type monochromator and imaging properties of the MANDOLINE filter", in Ultramicroscopy, **vol. 110**, no. 8, July 2010, pp. 971-980

[2] *I Linert, M Zubek*, "Differential cross sections for electron impact vibrational excitation of molecular oxygen in the angular range 15°–180°", in J. Phys. B: At. Mol. Opt. Phys., **vol. 39**, no. 20, Oct. 2006, pp. 4087-4095

[3] *O. Sise, M. Dogan, I. Okur, A. Crowe*, "Electron-impact excitation of the ($2p^2$) D_1 and (2s2p) P_1^o autoionizing states of helium", in Phys. Rev. A, **vol. 84**, no. 2, Aug. 2011, pp. 022705

[4] *M. Escher, K. Winkler, O. Renault, N. Barrett*, "Applications of high lateral and energy resolution imaging XPS with a double hemispherical analyser based spectromicroscope", in J. Electron Spectrosc. Relat. Phenom., **vol. 178–179**, May 2010, pp. 303-316

[5] *P. Louette, A. Delage, D. Roy, P.A. Thiry R. Caudano*, "An interelectrode distance dependent fringing field correction for the hemispherical deflector analyzer", in J. Electron Spectrosc. Relat. Phenom., **vol. 52**, Apr. 1990, pp. 867-874

[6] *R. Herzog*, "Ablenkung von Kathoden- und Kanalstrahlen am Rande eines Kondensators, dessen Streufeld durch eine Blende begrenzt Ist", in Zeitschrift für Physik A Hadrons and Nuclei, **vol. 97**, 1935, pp.596-602

[7] *C. Oshima, R. Franchy, H. Ibach*, "Numerical-calculations of electron trajectories in the 127-degree analyzer using a position-sensitive detector under conditions of fringing fields", in Rev. Sci. Inst., **vol. 54**, no. 8, 1983, pp. 1042-1046

[8] *C. Oshima, R. Souda, M. Aono, Y. Ishizawa*, "Optimum angle of deflection electrodes of a cylindrical electrostatic analyzer", in Rev. Sci. Inst., **vol. 56**, no. 2, 1985, pp. 227-230

[9] *S. Nishigaki, S. Kanai*, "Optimization of the Herzog correction in the hemispherical deflector analyzer", in Rev. Sci. Instr., **vol. 57**, no. 2, Feb. 1986, pp. 225-228

[10] *K. Jost*, "Fringing field correction for 127° and 180° electron spectrometers", in J. Phys. E, **vol. 12**, 1979, pp.1001-1005

[11] *D. Q. Hu, K. T. Leung*, "SIMION study of the fringing field effects in deflector-type electrostatic electron-energy analyzers - a new flexible Jost-based correction scheme", in Rev. Sci. Inst., **vol. 66**, no. 4, Apr. 1995, pp. 2865-2870

[12] *E. P. Benis, T. J. M. Zouros*, "Improving the energy resolution of a hemispherical spectrograph using a paracentric entry at a non-zero potential", in Nucl. Inst. Meth. A, **vol. 440**, no. 2, Feb. 2000, pp. 462-465

[13] *T. J. M. Zouros, O. Sise, M. Ulu, M. Dogan*, "Using the fringing fields of a hemispherical spectrograph to improve its energy resolution", in Meas. Sci. Tech., **vol. 17**, no. 12, Dec. 2006, pp. N81-N86

[14] *O. Sise, T. J. M. Zouros, M. Ulu, M. Dogan*, "Novel and traditional fringing field correction schemes for the hemispherical analyser: comparison of first-order focusing and energy resolution", in Meas. Sci. Tech., **vol. 18**, no. 7, Jul. 2007, pp. 1853-1858

[15] *O. Sise, G. Martinez, T. J. M. Zouros, M. Ulu, M. Dogan*, "Fringing field optimization of hemispherical deflector analyzers using BEM and FDM", in J. Electron Spectrosc. Relat. Phenom., **vol. 177**, no. 1, Feb. 2010, pp. 42-51

[16] *T. Sagara, L. Boesten, S. Nishida, K. Okada*, "Resolution improvements for hemispherical energy analyzers", in Rev. Sci. Inst., **vol. 71**, no.11, Nov. 2000, pp. 4201-4207

[17] *D. Roy, J. D. Carette*, "Optimum deflection angle for cylindrical and spherical electrostatic spectrometer", in Appl. Phys. Lett., **vol. 16**, 1970, pp. 413-416

[18] *E. M. Purcell*, "The focusing of charged particles by a spherical condenser", in Phys. Rev., **vol. 54**, 1938, pp. 818-826

[19] *T. J. M. Zouros, E. P. Benis*, "The hemispherical deflector analyser revisited. I. Motion in the ideal 1/r potential, generalized entry conditions, kepler orbits and spectrometer basic equation", in J. Electron Spectrosc. Relat. Phenom., **vol. 125**, no. 3, Sep. 2002, pp. 221-248

[20] *R. E. Imhof, A. Adams, G. C. King, "Energy and time resolution of the 180 degrees hemispherical electrostatic analyser", in J. Phys. E: Sci. Instrum., **vol. 9**, no.2, 1976, pp. 138-142*

[21] *K. Rossnagel, L. Kipp, M. Skibowski, S. Harm*, "A high performance angle-resolving electron spectrometer", in Nucl. Inst. Meth. A, **vol. 467**, no. 2, Jul. 2001, pp. 1485-1488